

Signatures of chiral symmetry restoration in dilepton production

Chihiro Sasaki¹

¹*Institute of Theoretical Physics, University of Wrocław, PL-50204 Wrocław, Poland*

(Dated: December 18, 2019)

We study the structural change of the vector spectral function and integrated production rates of dileptons in the presence of the chiral mixing induced exclusively at finite density. The mixing produces multiple bumps and peaks around the vacuum masses of the ρ, ω and ϕ resonances in the spectral function. The arising modification becomes pronounced when the mass difference between parity partners decreases. In particular, the emergent enhancement around the vacuum ϕ meson in the production rates serves as an excellent signature of the partially-restored chiral symmetry in heavy-ion collisions.

I. INTRODUCTION

The role of dynamical chiral symmetry breaking has been extensively explored in the context of relativistic heavy-ion collisions and the interior of compact stars [1–5]. A number of potential signatures of the restoration of chiral symmetry has been proposed in literature, whereas no conclusive evidence has been observed in experiment. Dileptons are one of the promising probes since a virtual photon can propagate in a medium without disturbance. The light vector mesons directly couple to the electromagnetic current correlator which is the central ingredient in dilepton production. An enhancement of the dilepton spectra below the ρ/ω resonances observed at the CERN SPS is a strong evidence that the vector mesons modify their properties in the medium [6].

The restoration of chiral symmetry is identified by the current-current correlation functions degenerate in opposite parity channels. It is characteristic in hot/dense matter that the pionic interaction yields a mixing of the vector with the axial-vector correlator. At low temperature or density, this is expressed as a model-independent theorem [7–9]. Some systematic calculations at finite temperature exist via the theorem [10, 11] and in a chiral reduction formalism [12]. In Ref. [13], it was shown that at finite temperature the chiral symmetry restoration forces the chiral mixing to vanish within a chiral effective theory of the ρ, a_1 mesons and the pion. The same trend is found in Ref. [14] where the in-medium axial-vector spectral function was constructed, via the Weinberg sum rules [15], from the vector current correlator that describes the dilepton data. There a substantial mass drop of the a_1 to the ρ mass and a width broadening toward the chiral symmetry restoration were reported.

In contrast to the above mixing induced by pion loops, there exists a new class of the chiral mixing that modifies the dispersion relations of the vector and axial-vector mesons at finite density. This mixing was shown to emerge in the low-energy effective theory of QCD based on the AdS/CFT correspondence [16]. Its phenomenological impact in dense QCD matter is a significant change of the vector spectrum which may lead to multiple bumps and peaks in dilepton rates at a few times of the normal nuclear matter density whereas assumed

that the mesons do not change their masses [17].

In this paper, we introduce the order parameter as a function of temperature and chemical potential to the vector current correlator in the presence of the density-induced mixing and study a possible signal of partial restoration of chiral symmetry to be verified in dilepton measurement. A special emphasis is put on the competition between the chiral mixing and the mass degeneracy of the parity partners. It is shown that decreasing the mass difference reinforces the structural change of the spectral function and this persists in the integrated dilepton rate even with a marginal strength of the mixing.

II. CHIRAL MIXING IN DENSE MATTER

At finite baryon density, charge-conjugation invariance is explicitly violated whereas parity invariance remains intact. The chiral Lagrangian thus includes a term

$$\mathcal{L}_{\text{mix}} = 2c \epsilon^{0\mu\nu\lambda} \text{tr} [\partial_\mu V_\nu \cdot A_\lambda + \partial_\mu A_\nu \cdot V_\lambda], \quad (2.1)$$

for the vector V_μ and the axial-vector A_μ mesons with the total anti-symmetric tensor $\epsilon^{0123} = 1$ as well as a mixing parameter c . The mixing yields the modified dispersion relations for the transverse polarizations [16]

$$p_0^2 - \vec{p}^2 = \frac{1}{2} \left[m_V^2 + m_A^2 \pm \sqrt{(m_A^2 - m_V^2)^2 + 16c^2 \vec{p}^2} \right], \quad (2.2)$$

with the lower sign for the vector and the upper one for the axial-vector mesons. The longitudinal modes obey the standard dispersion relation, $p_0^2 - \vec{p}^2 = m_{V,A}^2$.

In a model based on AdS/CFT at finite baryon chemical potential [16], the mixing strength c possesses an explicit dependence on the baryon density ρ_B and takes a rather large value $c \simeq 1$ GeV at the normal nuclear matter density ρ_0 . This results in the onset of vector condensation at a density slightly above ρ_0 , which is an apparent drawback of large N_c since the known property of nuclear matter excludes this possibility under a realistic setup with $N_c = 3$. This strongly suggests a non-trivial contribution as $1/N_c$ corrections, which may change the mixing strength quantitatively. The value of c can be determined in the standard chiral approach by

replacing Eq. (2.1) with the $\omega\rho a_1$ term that arises from the gauged Wess-Zumino-Witten (WZW) action [18]

$$\mathcal{L}_{\omega\rho a_1} = g_{\omega\rho a_1} \langle \omega_0 \rangle \epsilon^{0\mu\nu\lambda} \text{tr} [\partial_\mu V_\nu \cdot A_\lambda + \partial_\mu A_\nu \cdot V_\lambda], \quad (2.3)$$

where the iso-scalar ω field is replaced with its expectation value, $\langle \omega_0 \rangle = g_{\omega NN} \cdot \rho_B / m_\omega^2$, obtained in the conventional Walecka model. With empirical numbers, one finds the mixing strength $c = g_{\omega\rho a_1} \langle \omega_0 \rangle \simeq 0.1$ GeV at ρ_0 [17]. Although the weak mixing has little importance in the vector-current correlation function at ρ_0 , a distinct modification emerges at higher density leading to a stronger mixing $c \simeq 0.3$ GeV in the correlator and consequently in production rates of a lepton pair [17]. Note that no further term that changes the dispersion relation appears from the WZW action by replacing ω_μ with its expectation value. Induced interactions will modify the masses and widths via loop diagrams.

Whereas the mixing effect is expected to become more important at higher density, a crucial question to be answered is how the signals of the partial restoration of chiral symmetry would emerge in observables. Expanding the dispersion relation (2.2) for a small momentum \vec{p} , we readily see

$$p_0^2 \simeq m_{A,V}^2 + \left(1 \pm \frac{4c^2}{m_A^2 - m_V^2} \right) \vec{p}^2, \quad (2.4)$$

where the second term in the parentheses becomes enhanced as the mass difference between the parity partners decreases even with a marginal strength c . The above expression breaks down when the mass splitting $m_A^2 - m_V^2$ becomes small, so that a self-consistent determination of both $m_{A,V}$ and c is necessary to get a qualitative insight into the relevance of the mixing effect.

The mixing strength c and the meson masses $m_{V,A}$ in general carry certain medium effects that are inherently related to each other, and it requires a suitable extension of the previous study to determine those parameters in a self-consistent way. We begin with the vector and axial-vector current correlators in matter

$$G_{V,A}^{\mu\nu}(p_0, \vec{p}) = P_L^{\mu\nu} G_{V,A}^L(p_0, \vec{p}) + P_T^{\mu\nu} G_{V,A}^T(p_0, \vec{p}), \quad (2.5)$$

with the polarization tensors

$$\begin{aligned} P_{T,\mu\nu} &= g_{\mu i} \left(\delta_{ij} - \frac{\vec{p}_i \vec{p}_j}{\vec{p}^2} \right) g_{j\nu}, \\ P_{L,\mu\nu} &= - \left(g_{\mu\nu} - \frac{p_\mu p_\nu}{p^2} \right) - P_{T,\mu\nu}. \end{aligned} \quad (2.6)$$

The longitudinal and transverse parts are expressed as [17]

$$\begin{aligned} G_V^L &= \left(\frac{g_V}{m_V} \right)^2 \frac{-s}{D_V}, & G_V^T &= \left(\frac{g_V}{m_V} \right)^2 \frac{-s D_A + 4c^2 \vec{p}^2}{D_V D_A - 4c^2 \vec{p}^2}, \\ G_A^L &= \left(\frac{g_A}{m_A} \right)^2 \frac{-s}{D_A}, & G_A^T &= \left(\frac{g_A}{m_A} \right)^2 \frac{-s D_V + 4c^2 \vec{p}^2}{D_V D_A - 4c^2 \vec{p}^2}, \end{aligned} \quad (2.7)$$

with $s = p_0^2 - \vec{p}^2$ and the coupling of the vector/axial-vector meson to the corresponding current $g_{V,A}$ as well as the propagator inverse without the mixing $D_{V,A} = s - m_{V,A}^2 + i m_{V,A} \Gamma_{V,A}(s)$. The spin-averaged correlators are defined by $G_{V,A} = \frac{1}{3} (G_{V,A}^L + 2G_{V,A}^T)$. The labels (V, A) refer to the iso-vector states (ρ, a_1) and the iso-singlet states $(\omega, f_1(1285))$ and $(\phi, f_1(1420))$.

Phenomenology of the pseudo-scalar and vector mesons is well described in the non-linear chiral Lagrangian based on the generalized hidden local symmetry (GHLS) [18–20]. The vector and axial-vector meson masses are related via the pion decay constant f_π as

$$m_A^2 - m_V^2 = g^2 \frac{m_A^2}{m_V^2} f_\pi^2 \equiv \delta m^2, \quad (2.8)$$

with the gauge coupling g . Thus, the mass difference δm serves as the order parameter of spontaneous chiral symmetry breaking. In order to introduce a non-trivial medium effect that induces a chiral phase transition, we shall replace f_π with the in-medium expectation value of the sigma field $\langle \sigma \rangle$ computed in the standard linear sigma model. We note that vanishing δm leads to $m_A \rightarrow m_V$, $\Gamma_A \rightarrow \Gamma_V$ and $g_A \rightarrow g_V$, so that the spectral functions become identical in the vector and axial-vector channels for non-vanishing c .

For an illustrative calculation, we employ the nucleon parity-doublet model to obtain medium profiles of the sigma and omega expectation values in the mean field approximation, where the lowest nucleon and its negative-parity counterpart $N(1535)$ play the essential role in describing the nuclear ground state [21, 22]. The model has been extended further by introducing the confinement nature on top of the chiral dynamics and confronted with the properties of neutron stars [23]. In Fig. 1, we show the resultant mass-splitting and the chiral mixing at temperature $T = 50$ MeV as functions of baryon chemical potential μ_B . It is characteristic of the nucleon parity doublet model that the VEV of the sigma field drops twice, at the liquid-gas (LG) transition and at the chiral phase transition/crossover at zero temperature [21]. When the model is applied to finite temperature, the first-order LG transition becomes a crossover via a second-order critical point. One still sees its remnant in the VEV as an abrupt change at a relatively low chemical potential μ_B [22]. The model with the parameters constrained by the maximum masses and the compactness of the neutron stars in [23] yields a chiral crossover at $\mu_B \simeq 1.05$ GeV (equivalently the net baryon density $\rho_B \simeq 2.5 \rho_0$), at which the lowest nucleon and the $N(1535)$ become nearly degenerate. That way, we can handle the low-lying parity doublers both in the meson and baryon sectors on the equal footing.

In the subsequent calculations, we shall set the vector meson mass to its vacuum value at any T and μ_B for simplicity, and this prescription is supported in line with the known phenomenology as well [2]. Thus, the axial-vector mass $m_A = \sqrt{m_V^2 + \delta m^2}$ and the decay width

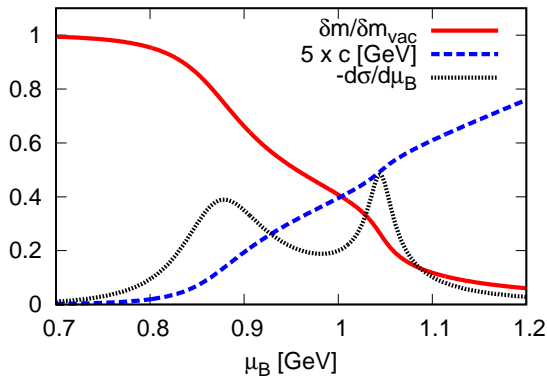


FIG. 1: The mass difference between the vector and axial-vector mesons δm normalized its vacuum value, the chiral mixing c and the μ_B -derivative of the order parameter at fixed temperature $T = 50$ MeV as functions of baryon chemical potential μ_B . The μ_B profiles of the two mean fields, $\langle\sigma_q\rangle$ and $\langle\omega_0\rangle$ are taken from [23]

$\Gamma_A(m_V, m_A)$ vary with respect to T and μ_B according to δm in the spectral function (2.7). Also, we use the form of the vacuum decay widths for the ρ and a_1 mesons [17]

$$\begin{aligned}\Gamma_\rho(s) &= \Theta(s - 4m_\pi^2) \frac{m_\rho}{\sqrt{s}} \left(\frac{s - 4m_\pi^2}{m_\rho^2 - 4m_\pi^2} \right)^{3/2} \Gamma_\rho, \\ \Gamma_\rho &= \frac{1}{6\pi m_\rho^2} \left(\frac{m_\rho^2 - 4m_\pi^2}{4} \right)^{3/2} g_{\rho\pi\pi}^2, \\ \Gamma_{a_1}(s) &= \Theta(s - (m_\rho + m_\pi)^2) \frac{g^2}{8\pi m_{a_1}^2} \left[g^2 f_\pi^2 + \frac{m_{a_1}^2 - m_\rho^2}{12m_{a_1}^2} s \right. \\ &\quad \times \left(1 - \frac{(m_\rho + m_\pi)^2}{s} \right) \left(1 - \frac{(m_\rho - m_\pi)^2}{s} \right) \left. \right] \\ &\quad \times \sqrt{1 - \frac{(m_\rho + m_\pi)^2}{2s}} \sqrt{1 - \frac{(m_\rho - m_\pi)^2}{2s}}, \quad (2.9)\end{aligned}$$

with the parameter $g = 6.61$ [13]. We take the following values at $T = \mu_B = 0$ for our calculations: $f_\pi = 92.4$ MeV, $m_\pi = 0.14$ GeV, $m_\rho = 0.77$ GeV, $g_\rho = 0.119$ GeV², $g_{\rho\pi\pi} = 6$ and $m_{a_1} = 1.26$ GeV [25], which lead to the on-shell decay widths, $\Gamma_\rho(s = m_\rho^2) = 0.15$ GeV and $\Gamma_{a_1}(s = m_{a_1}^2) = 0.33$ GeV.

In Eq.(2.9) we deal with the mass m_{a_1} and the order parameter $f_\pi = \langle\sigma\rangle$ as in-medium quantities, thus the width Γ_{a_1} carries the medium effect corresponding to partial restoration of the chiral symmetry. One readily finds that the Γ_{a_1} vanishes as $f_\pi \rightarrow 0$, consistently to the a_1 carrying the equal mass to the ρ meson when the chiral symmetry gets restored. Therefore, in order to ensure the degenerate current correlators, $G_V = G_A$, we must include an additional term to Eq. (2.9) which contributes to the total a_1 width with the equal strength to the Γ_ρ . Here the scalar degree of freedom comes in.

In the linear sigma model, the axial-vector meson decays into the lowest scalar meson σ and pion. At the chiral restoration, the scalar meson mass becomes equal to the pion mass, so that the decay rate is expected to be $\Gamma_{a_1 \rightarrow \sigma\pi} = \Gamma_{\rho \rightarrow 2\pi}$. Therefore, we adopt the schematic parameterizations

$$\begin{aligned}\Gamma_{a_1}(s) &= \Gamma_{a_1 \rightarrow \rho\pi}(s) + \delta\Gamma_{a_1}(s), \\ \delta\Gamma_{a_1}(s) &= \Theta(s - 4m_\pi^2) \Gamma_\rho \left[1 - \left(\frac{\langle\sigma\rangle}{\langle\sigma\rangle_{\text{vac}}} \right)^2 \right] \quad (2.10)\end{aligned}$$

The chiral mixing between ω - $f_1(1285)$ and ϕ - $f_1(1420)$ can be introduced in a straightforward way [17]. We employ the constant-width approximation of narrow peaked mesons above threshold: $\Gamma_\omega = 8.49$ MeV, $\Gamma_\phi = 4.26$ MeV, $\Gamma_{f_1(1285)} = 24.3$ MeV and $\Gamma_{f_1(1420)} = 54.9$ MeV [25], with the kinematical constraints

$$\begin{aligned}\Gamma_\omega(s) &= \Theta(s - 9m_\pi^2) \Gamma_\omega, \\ \Gamma_\phi(s) &= \Theta(s - 4m_K^2) \Gamma_\phi, \\ \Gamma_{f_1(1285)}(s) &= \Theta(s - 16m_\pi^2) \Gamma_{f_1(1285)}, \\ \Gamma_{f_1(1420)}(s) &= \Theta(s - (m_\pi + 2m_K)^2) \Gamma_{f_1(1420)}. \quad (2.11)\end{aligned}$$

The coupling constants to the vector current are related to g_ρ via chiral symmetry, so that

$$g_\omega = \frac{1}{3} \frac{m_\omega^2}{m_\rho^2} g_\rho, \quad g_\phi = \frac{\sqrt{2}}{3} \frac{m_\phi^2}{m_\rho^2} g_\rho. \quad (2.12)$$

We employ the same parameterizations for $\delta\Gamma_{f_1}$ as in Eq. (2.10).

It may not be appropriate to naively replace $\langle\omega_0\rangle$ with $\langle\phi_0\rangle$ to obtain the mixing between the ϕ and $f_1(1420)$ states since the mean-field calculations typically yield a $\langle\bar{s}s\rangle$ decreasing in a much milder way than the light-quark condensate. This results in a significant delay of vanishing δm which contradicts the vector screening mass of the $\bar{s}s$ state seen in lattice simulations [24]. There the screening masses exhibit a substantial modification at around the pseudo-critical temperature and this arises nearly independent of the quark-flavor content. Therefore, we will not proceed to a three-flavored parity doublet model, but rather impose the same critical behavior of the meson masses as the lattice observation. To this end, the simplest way is to assume that the modification of δm for the ϕ and $f_1(1420)$ is dominated by the two-flavor physics. In the subsequent calculations, we will set at the chiral crossover $\delta m / \delta m_{\text{vac}} = 0.36$ for the strange vector mesons, whereas the two-flavored parity doublet model yields $\delta m / \delta m_{\text{vac}} = 0.26$ for the light vector states. The same re-scaling is applied to the expectation value of $\langle\phi_0\rangle$.

III. VECTOR SPECTRAL FUNCTION

To illustrate the competition between the density-induced mixing and chiral symmetry restoration, we de-

fine the vector spectral function as the imaginary part of the current correlator, $\text{Im}G_V$, for a given three-momentum \vec{p} . The characteristic feature with the chiral mixing is that the longitudinal part of the correlator is peaked at the vacuum mass of the vector state, whereas the transverse parts are modified by the transverse vector-meson with a shifted mass downward and the transverse axial-vector with a shifted mass upward. Consequently, the vector spectral function exhibits three bumps in hadronic phase if the mixing strength is sufficiently large [17]. As the system gradually approaches the chiral symmetry restoration in dense matter, those bumps and peaks are supposed to change their locations according to the dispersion relations Eq.(2.2).

In Fig. 2 we show the vector spectral function at $T = 50$ MeV in the ρ - ω and ϕ channels using Eq. (2.7) with $|\vec{p}| = 0.5$ GeV and the condensates shown in Fig. 1. In the ρ - ω channel, the distinct peak of the longitudinal ω meson stays at any μ_B whereas its strength is decreased because of the mixing effect. At $\delta m/\delta m_{\text{vac}} = 0.7$, the system remains far from the chiral symmetry restoration and the mixing effect with $c \simeq 34$ MeV is totally irrelevant. At higher μ_B , the mixing sets in because of decreasing $\delta m/\delta m_{\text{vac}}$ and the spectrum exhibits multiple bumps of the transverse polarizations, which changes the locations in μ_B . Especially, the transverse ρ yields a substantial contribution near the chiral crossover and the spectrum becomes enhanced at small \sqrt{s} . The aforementioned structure with the three bumps is best preserved in the ϕ channel at $\delta m/\delta m_{\text{vac}} = 0.26$. The most-left peak of the transverse ϕ shifts its position to lower \sqrt{s} as μ_B is increased. At some point, it meets the threshold and becomes cut off from the spectrum. This will lead to a two-peak structure at a smaller $\delta m/\delta m_{\text{vac}}$. We emphasize that the distinct modification in the spectral function disappears when the masses of the axial-vector mesons are frozen to be constant, since the mixing c is not very strong at any μ_B considered in this study and is insufficient to modify the propagators. Therefore, the drastic change seen in Fig. 2 is the direct consequence of the chiral symmetry restoration.

It is a straightforward and intriguing application to calculate the production rate of a lepton pair emitted from dense matter via a virtual photon. The differential rate in a medium at finite T and μ_B is given in terms of the imaginary part of the vector current correlator [2]

$$\frac{dN}{d^4p}(p_0, \vec{p}; T, \mu_B) = \frac{\alpha^2}{\pi^3 s} \frac{\text{Im}G_V(p_0, \vec{p}; T, \mu_B)}{e^{p_0/T} - 1}, \quad (3.1)$$

with $\alpha = e^2/4\pi$ the electromagnetic coupling constant. The three-momentum integrated rate is given by

$$\frac{dN}{ds}(s; T, \mu_B) = \int \frac{d^3\vec{p}}{2p_0} \frac{dN}{d^4p}(p_0, \vec{p}; T, \mu_B). \quad (3.2)$$

In Fig. 3, the integrated rate in the range of $0 \leq |\vec{p}| \leq 1$ GeV at $T = 50$ MeV is presented for $\mu_B/\mu_B^c = 0.75$ and 1.0. The characteristic structure remains there even af-

ter the \vec{p} -integral is performed, although somewhat weakened. The modified ρ and ω mesons yield a significant enhancement in low \sqrt{s} region, and the axial-vector counterpart of the ϕ meson produces one additional peak around $\sqrt{s} \sim 1.1$ GeV near the chiral symmetry restoration. The transverse ϕ state appears rather close to the longitudinal polarization, and thus the entire spectrum becomes broadened.

In the above calculations, in-medium broadening of the widths were not taken into account. The presence of hot and dense matter strongly modifies the shape of the vector spectral function [2]. In fact, a systematic treatment of the in-medium ρ meson successfully describes the dilepton data of the NA60 Collaboration in heavy-ion collisions at CERN SPS [26], where the characteristic baryon-induced interactions play the central role. Thus, in a more realistic calculation with the chiral mixing, such broadened widths may screen the additional bumpy structure of the spectrum, especially in the ρ - ω channel. On the other hand, the ϕ -meson spectrum receives much weaker modifications and the ϕ remains a well-defined narrow resonance in a medium [27]. We therefore anticipate that the modification of the vector spectrum in the ϕ channel serves as a convincing signal of the chiral symmetry restoration. The additional peaks of the modified ϕ and $f_1(1420)$ states will lead to the two bumps, one is below and another is above the vacuum ϕ meson mass, in the dilepton rates by summing up the evolution history of the created matter. We note that the transverse polarizations change their masses systematically to lower values as μ_B increases, and at some point the lower peak is cut off at the $2m_K$ threshold. Therefore, the number of bumps actually seen in the rate depends on the chemical potential μ_B .

As an illustration, we show the rate at the chiral restoration point $\delta m/\delta m_{\text{vac}} = 0.26$ with a larger width of the ϕ meson than its vacuum value by factors of 3 and 5 in Fig. 4. The peak of the longitudinal polarization is clearly suppressed and the entire shape is much broadened, as expected. Whereas, the enhancement below and above the vacuum ϕ meson clearly survives. Thus, there remains a good chance to observe a trace of the chiral symmetry restoration via the chiral mixing in more realistic calculations of the dilepton rate if the matter is sufficiently dense and cold.

IV. CONCLUSIONS

We have studied the consequences of the density-induced chiral mixing in the vector spectral function and the dilepton production rate, with a special emphasis on ensuring the restoration of chiral symmetry. The absence of charge-conjugation invariance at finite chemical potential naturally leads to the modified dispersion relations for the transverse polarizations of the vector and axial-vector mesons. Multiple bumps and peaks arise in the spectral function and they gradually change the lo-

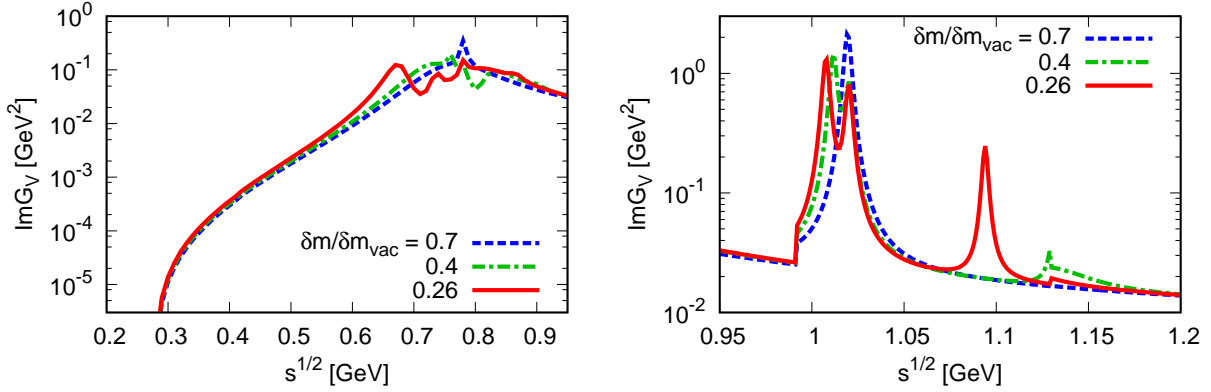


FIG. 2: The vector spectral function with $|\vec{p}| = 0.5$ GeV at $T = 50$ MeV in the ρ - ω (left) and ϕ (right) channels for $\delta m/\delta m_{\text{vac}} = 0.7, 0.4$ and 0.26 .

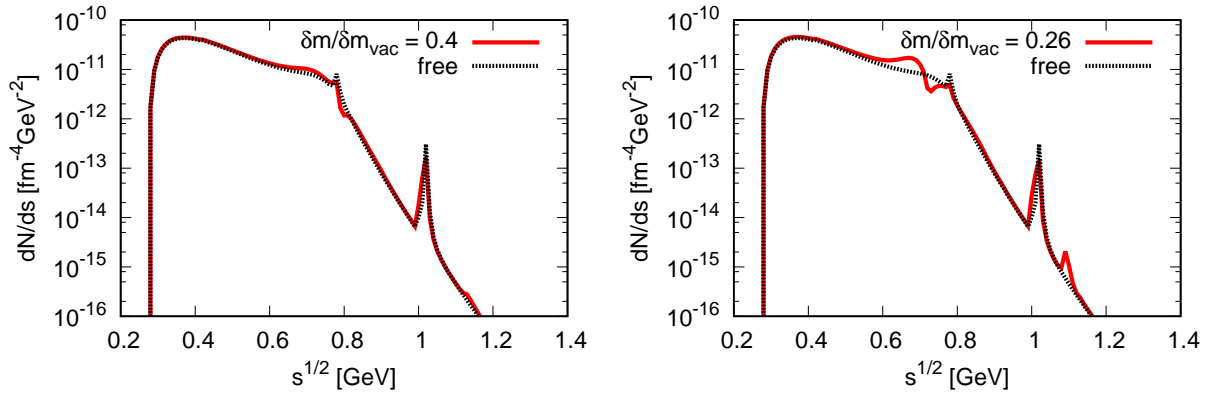


FIG. 3: The dilepton production rate at $T = 50$ MeV for $\delta m/\delta m_{\text{vac}} = 0.4$ (left) and 0.26 (right).

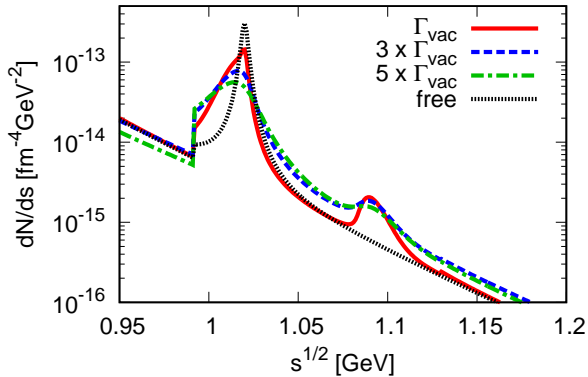


FIG. 4: The dilepton production rate at $T = 50$ MeV for $\delta m/\delta m_{\text{vac}} = 0.26$ with various decay widths of the ϕ meson.

fications according to the onset of the chiral symmetry restoration.

It is striking that, even with a marginal strength of the mixing, $c \sim 0.1$ GeV, decreasing the order parameter δm

reinforces the structural change of the spectral function. This is in a sharp contrast to the scenario without the mass degeneracy [17]. Therefore, the arising enhancement around the ρ, ω and ϕ resonances in the dilepton rates serves as a clear signature of the restored chiral symmetry. Especially, the ϕ meson and its axial-vector counterpart carry much more promising signals than the ρ and a_1 states since the ϕ likely remains a well-defined narrow resonance in a hot/dense medium. This will be an excellent signal of the chiral symmetry restoration to be verified in heavy-ion collisions at FAIR, NICA and J-PARC.

In our calculations, the in-medium widths of the axial-vector mesons were minimally modified such that the current correlation functions in the vector and axial-vector channels coincide at the restoration point. Hadronic many-body approaches will certainly modify the spectral function quantitatively, and it is mandatory to determine the axial-vector decay rates more precisely near the chiral symmetry restoration on top of the chiral mixing. Despite the simplifications made in our calculations, the strategy does not rely on the detailed prescriptions to

handle the many-body dynamics. In fact, the two current correlators must coincide at the restoration, $G_V = G_A$, with the total in-medium widths $\Gamma_{V,A}^*$ independently on how they are evaluated. Further study on the vector spectral function including major baryon-induced effects and the production of the ϕ meson in dense matter is a work in progress.

Acknowledgments

I acknowledge stimulating discussions with W. Bro-niowski, T. Galatyuk, K. Redlich, P. Salabura and

N. Xu. I also thank Michal Marczenko for providing me the condensates calculated in his model. This work has been partly supported by the Polish Science Foundation (NCN) under Maestro Grant No. DEC-2013/10/A/ST2/00106 and OPUS Grant No. 2018/31/B/ST2/01663.

-
- [1] R. S. Hayano and T. Hatsuda, *Rev. Mod. Phys.* **82**, 2949 (2010).
 - [2] R. Rapp, J. Wambach and H. van Hees, *Landolt-Bornstein* **23**, 134 (2010).
 - [3] A. Bazavov *et al.* [HotQCD Collaboration], *Phys. Rev. D* **86**, 034509 (2012).
 - [4] K. Fukushima and C. Sasaki, *Prog. Part. Nucl. Phys.* **72**, 99 (2013).
 - [5] A. Andronic, P. Braun-Munzinger, K. Redlich and J. Stachel, *Nature* **561**, no. 7723, 321 (2018).
 - [6] R. Arnaldi *et al.* [NA60 Collaboration], *Phys. Rev. Lett.* **96**, 162302 (2006).
 - [7] M. Dey, V. L. Eletsky and B. L. Ioffe, *Phys. Lett. B* **252**, 620 (1990).
 - [8] B. Krippa, *Phys. Lett. B* **427**, 13 (1998).
 - [9] G. Chanfray, J. Delorme and M. Ericson, *Nucl. Phys. A* **637**, 421 (1998).
 - [10] E. Marco, R. Hofmann and W. Weise, *Phys. Lett. B* **530**, 88 (2002).
 - [11] M. Urban, M. Buballa and J. Wambach, *Phys. Rev. Lett.* **88**, 042002 (2002).
 - [12] K. Dusling, D. Teaney and I. Zahed, *Phys. Rev. C* **75**, 024908 (2007).
 - [13] M. Harada, C. Sasaki and W. Weise, *Phys. Rev. D* **78**, 114003 (2008).
 - [14] P. M. Hohler and R. Rapp, *Phys. Lett. B* **731**, 103 (2014).
 - [15] S. Weinberg, *Phys. Rev. Lett.* **18**, 507 (1967).
 - [16] S. K. Domokos and J. A. Harvey, *Phys. Rev. Lett.* **99**, 141602 (2007).
 - [17] M. Harada and C. Sasaki, *Phys. Rev. C* **80**, 054912 (2009).
 - [18] N. Kaiser and U. G. Meissner, *Nucl. Phys. A* **519**, 671 (1990).
 - [19] M. Bando, T. Kugo and K. Yamawaki, *Phys. Rept.* **164**, 217 (1988).
 - [20] M. Harada and C. Sasaki, *Phys. Rev. D* **73**, 036001 (2006).
 - [21] D. Zschesche, L. Tolos, J. Schaffner-Bielich and R. D. Pisarski, *Phys. Rev. C* **75**, 055202 (2007).
 - [22] C. Sasaki and I. Mishustin, *Phys. Rev. C* **82**, 035204 (2010).
 - [23] M. Marczenko, D. Blaschke, K. Redlich and C. Sasaki, *Universe* **5**, no. 8, 180 (2019).
 - [24] M. Cheng *et al.*, *Eur. Phys. J. C* **71**, 1564 (2011).
 - [25] M. Tanabashi *et al.* [Particle Data Group], *Phys. Rev. D* **98**, no. 3, 030001 (2018).
 - [26] H. van Hees and R. Rapp, *Phys. Rev. Lett.* **97**, 102301 (2006).
 - [27] R. Rapp, *Phys. Rev. C* **63**, 054907 (2001).